Article

Not peer-reviewed version

Effect of Amino-Functionalized POSS on Structure-Property Relationships of Thermostable Hybrid Cyanate Ester Resin Based Nanocomposites

Olga Grigoryeva * , Alexander Fainleib , Olga Starostenko , Diana Shulzhenko , Agustin Rios de Anda , Fabrice Gouanvé , Eliane Espuche , Daniel Grande

Posted Date: 15 November 2023

doi: 10.20944/preprints202311.0954.v1

Keywords: cyanate ester resin; amino-POSS; polycyanurate; glass transition temperature; thermal stability; gas permeability

Research

Effect of Amino-Functionalized POSS on Structure-Property Relationships of Thermostable Hybrid Cyanate Ester Resin Based Nanocomposites

Olga Grigoryeva [1,*], Alexander Fainleib [1], Olga Starostenko [1], Diana Shulzhenko [1], Agustin Rios de Anda [2], Fabrice Gouanve [3], Eliane Espuche [3] and Daniel Grande [2]

[1] Institute of Macromolecular Chemistry, National Academy of Sciences of Ukraine, 48, Kharkivske shose, Kyiv 02160, Ukraine
[2] Univ Paris Est Creteil, CNRS, Institut de Chimie et des Matériaux Paris-Est, UMR 7182, 2 rue Henri Dunant, 94320, Thiais, France
[3] Univ Claude Bernard Lyon 1, CNRS, Ingénierie des Matériaux Polymères, UMR 5223, 15 Boulevard André Latarjet, 69622, Villeurbanne, France
* Correspondence: olgagrigoryeva@i.ua

Abstract: Nanocomposites of cyanate ester resin (CER) filled with three different reactive amino-functionalized polyhedral oligomeric silsesquioxane (POSS) were synthesized and characterized. The addition of a small quantity (0.1 wt.%) of amino-POSS chemically grafted to the CER network led to increasing thermal stability of CER matrix. A significant increase of the glass transition temperature, T_g (DSC data), and the temperature of α relaxation, T_α (DMTA data), by 45-55 °C of CER matrix with loading of nanofillers was evidenced. CER/POSS films exhibited a higher storage modulus than that of neat CER in the temperature range investigated. It was evidenced that CER/aminopropylisobutyl (APIB)-POSS, CER/*N*-phenylaminopropyl (*N*PAP)-POSS, and CER/aminoethyl aminopropylisobutyl (AEAPIB)-POSS nanocomposites induced a more homogenous α relaxation phenomenon with higher T_α values and an enhanced nanocomposite elastic behavior. Furthermore, CER/amino-POSS nanocomposites possessed higher specific surface area, gas permeability (CO_2, He), and diffusion coefficients (CO_2) values than those for neat CER, due to increasing free volume of the nanocomposites studied that is very important for their gas transport properties. Permeability grew respectively by about 2 (He) and 3.5-4 times (CO_2), and diffusion coefficient of CO_2 increased approximately twice for CER/amino-POSS nanocomposites in comparison with the neat CER network. The efficiency of amino-functionalized POSS in improving the thermal and transport properties of the CER/amino-POSS nanocomposites increased in a raw of reactive POSS containing one primary (APIB-POSS) < eight secondary (*N*PAP-POSS) < one secondary and one primary (AEAPIB-POSS) amino groups. APIB-POSS had the least strongly pronounced effect, since it could form covalent bonds with the CER network only by reaction of one $-NH_2$ group, while AEAPIB-POSS displayed the most highly marked effect, since it could easily be incorporated into the CER network *via* reaction of $-NH_2$ and –NH– groups with –O–C≡N groups from CER.

Keywords: cyanate ester resin; amino-POSS; polycyanurate; glass transition temperature; thermal stability; gas permeability

1. Introduction

Cyanate Ester Resins (CER) constitute a very attractive class of high-performance polymers, which differs from others by a very regular structure of the polymer networks, namely polycyanurates (PCNs), obtained by dicyanate polycyclotrimerization [1–5]. They have received much attention because of their unique combination of physical properties, including high thermal stability (> 400 °C), high glass transition temperature (> 270 °C), high fire-radiation and chemical resistance, low water absorption and low outgassing, high adhesion to different substrates, and excellent dielectric properties (ε = 2.64–3.11) [2–4]. As a result, CERs are currently used as structural or functional materials in aeronautics, space structures (composite strakes, fins, nose radar domes, heat shields), printed circuit boards, as well as adhesives [6]. The following companies manufacture

 doi:10.20944/preprints202311.0954.v1

CERs for these applications: Cytec Aerospace Materials, Hexcel, Huntsman Advanced Materials, JFC Technologies, Lonza, Henkel, TenCate Advanced Composites. However, like for most thermosets, their main drawback is brittleness. To overcome this limitation, modification of CERs has been developed over the past decades, and it is still of great interest. CERs can be modified by many different additives, such as engineering thermoplastics, elastomers, or reactive oligomers [2–5,7–14] with formation of semi-IPNs, IPNs and hybrid networks [7–34]. Improvement of mechanical properties can thus be attained, due to microphase-separated morphology generation, and especially in the case of a co-continuous morphology.

Unfortunately, the latter improvement is often achieved at the expense of thermal stability. This deficiency is remedied by the synthesis of nanocomposites of CER with montmorillonite (MMT) [35–40], carbon nanotubes [41,42], nanostructured aluminum borate [43], ZnO [44], ZrW_2O_8 [45], nanosilica [46–48], polyhedral oligomeric silsesquioxane (POSS) [49–64], and other nanofillers. The most pronounced effect on mechanical and thermal properties of CERs is achieved when nanoparticles with organically modified surface are used, as they may react with polymer networks.

POSS represent cage structures with the formula $(RSiO_{1.5})_n$ where n = 8, 10, 12 and R is hydrogen, reactive, or non-reactive organic groups. Each silicon atom is bonded to three oxygen atoms in a cage and to a single R substituent out of cage. These substituents improve compatibility of POSS molecules with polymers or monomers. In the case of reactive R, 3-D POSS molecules with diameters of 1-2 nm may graft chemically to polymer structures. New hybrid organic–inorganic CER-based thermosets with hydroxyl- [49,51,52,55], amino- [50,53] or epoxy-functionalized [59–64] POSS units have thus been obtained with improved thermal and mechanical properties.

Recently, thermostable nanocomposites based on densely crosslinked CER doped by 0.01–10 wt.% epoxycyclohexyl-functionalized POSS (ECH-POSS) were synthesized and characterized using TEM, SAXS, EDXS, FTIR, DSC, DMA, TGA, far-IR, and creep rate spectroscopy techniques [60,61]. It was revealed that ultra-low POSS contents (<<1 wt.%), covalently embedded into CER network substantially changed its nanostructure and properties [60,61,64]. This resulted in changing network dynamics, increasing glass transition temperatures by 20–50 ^{o}C, enhancing high temperature elastic and creep resistance properties, and increasing thermal stability under inert atmosphere at T < 400 ^{o}C. The effects decreased, or even became zero or negative, while increasing POSS content, especially from 2 to 10 wt.%, due to arising the structural nanorod- or platelet-like formations and POSS enriched nanodomains. At ultra-low POSS contents, the data obtained suggested basically molecular POSS dispersion, their quasi-periodic spatial distribution in the matrix, and not only chemical modifying CER network but also the possible manifestation of the enhanced long-range action of the "constrained dynamics" effect.

The aim of the present work is to synthesize and investigate the structure-properties relationships for nanocomposites of CER filled with amino-functionalized POSS of different reactivities, *i.e.* possessing different numbers of primary and/or secondary amino-groups. We intend to study the effect of amino-functionalized POSS nanoparticles on phase structure, morphology, physical properties, and gas permeability of the CER/amino-POSS films elaborated. Amino groups are very reactive towards cyanate groups [2,65,66], therefore during mixing of the functionalized POSS nanoparticles with CER, the nanoparticles may react and be chemically incorporated into the CER network [60,61,64].

We expect that reactive amino-functionalized POSS cage structures evenly distributed in CER networks will improve their thermal and mechanical properties as well as gas permeability for small molecules through the CER/amino-POSS polymer films, which will extend the areas of applications of such CER-based nanocomposites, especially in extreme conditions.

2. Materials and Methods

2.1. Materials

The CER network was formed using 1,1'-bis(4-cyanatophenyl) ethane (dicyanate ester of bisphenol E, DCBE), under the trade name PRIMASET® LECy, kindly supplied by Lonza

Preprints (www.preprints.org) | NOT PEER-REVIEWED | Posted: 15 November 2023 doi:10.20944/preprints202311.0954.v1

(Switzerland). POSS derivatives, *viz.*, aminopropylisobutyl POSS® (APIB-POSS), aminoethyl aminopropylisobutyl POSS® (AEAPIB-POSS), and *N*-phenylaminopropyl POSS® (*N*PAP-POSS) from Hybrid Plastics Inc. (Hattiesburg, MS, USA), were used as received. The chemical structures and basic physical characteristics for these components are given in **Table 1**.

2.2. Synthesis Procedure

The initial DCBE/POSS mixtures were first stirred with magnetic stirrer (1500 rpm) at $T \approx 65$ °C during 2 h for POSS dispersion and chemical grafting through the reaction between cyanate groups of CER and amino groups of POSS. Then, the mixtures obtained were poured into a PTFE-coated mold and cured over the temperature range from 25 °C to 300 °C with a heating rate of 0.5 °C/min. All polymer nanocomposites derived from DCBE were synthesized with a constant mass proportion of different amino-POSS equal to 0.1 wt.%.

2.3. Characterization Techniques

Dynamic mechanical thermal analysis (DMTA) was performed using a TA Instruments Q800 analyzer operating with 0.05 % of strain amplitude and a frequency of 1 Hz. The samples were heated from -150 °C to 320 °C at a heating rate of 3 °C/min. Loss modulus peaks corresponding to the α relaxation were deconvoluted with IgorPro 6.38 software. The surface of deconvoluted peaks was calculated *via* the MultiPeak 1.4 function of this software by fitting the peaks with Gaussian distribution functions. The molar mass between crosslinks M_c was then calculated according to Equation (1) [67]:

$$M_C = \frac{E'}{\phi RTf} \quad (1)$$

where E' is the elastic modulus taken at T_α + 50 °C, R is the ideal gas constant equal to 8.314 J/mol·K, $T = T_\alpha$ + 50 °C, f is the network functionality which for the studied samples was considered equal to 3, and ϕ is a factor linked to the network model. In this work, we considered the affine model best suitable for highly crosslinked polymers [68]. For this model $\phi = 1$.

Table 1. Chemical structure and physical characteristics of the components used.

Name	Chemical structure	Physical characteristics
Dicyanate ester of bisphenol E, DCBE	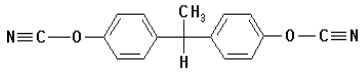	M = 264 g·mol^{-1} T_m = 29 °C T_b > 240 °C D_4^{20} = 1.18 g·cm^{-3} η = 75 mPa·s
Aminopropylisobutyl POSS, APIB-POSS	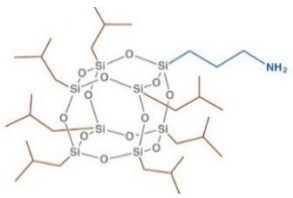	M = 875 g·mol^{-1} D_4^{20} = 1.16 g·cm^{-3} n_D^{20} = 1.46
Aminoethyl aminopropylisobutyl POSS, AEAPIB-POSS	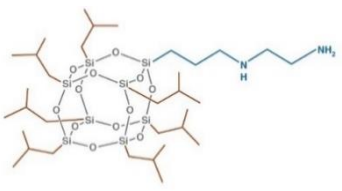	M = 918 g·mol^{-1} D_4^{20} =1.17 g·cm^{-3} n_D^{20} = 1.50

Preprints (www.preprints.org) | NOT PEER-REVIEWED | Posted: 15 November 2023 doi:10.20944/preprints202311.0954.v1

N-Phenylaminopropyl POSS, *N*PAP-POSS	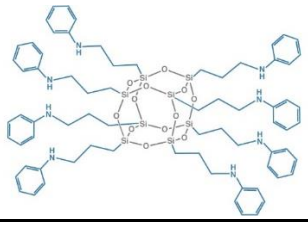	M = 1490 g·mol^{-1} D_4^{20} = 1.20 g·cm^{-3} n_D^{20} = 1.57

The nitrogen sorption measurements were carried out at 77 K (-196 °C) with a Micromeritics ASAP 2010 analyzer. The specific surface area (S) values were calculated using the Brunauer–Emmett–Teller (BET) method in the relative pressure (P/P_0) range from 0.05 to 0.3 by Equation (2) [69]:

$$S = {S_t}/{w} \quad (2)$$

where S_t is the total surface area derived from Equation (3), and w is the sample mass.

$$S_t = \frac{W_m \cdot N \cdot A_{cs}}{M} \quad (3)$$

where W_m is the mass of adsorbate as monolayer, N is Avogadro's number (6.02×10^{23} mol^{-1}), A_{cs} is the adsorbate cross sectional area (16.2 Å^2 for Nitrogen), and M is the molar mass of adsorbate.

The thermal stability of composites was determined by thermogravimetric analysis (TGA) using a Setaram SETSYS evolution 1750 thermobalance, with a platinum pan under 20 mL/min argon flow at a heating rate of 20 °C/min from 50 °C to 650 °C. The initial mass of the samples was equal to about 10 mg in all the cases.

Differential scanning calorimetry (DSC) with Perkin-Elmer Diamond DSC apparatus was used for estimating glass transition temperatures, T_g, at the half-height of a heat capacity step and glass transition onset temperatures, $T_{g\,onset}$, in the composites. The second scans with the heating rate of 40 °C/min over the temperature range from 20 to 350 °C in nitrogen atmosphere were performed. Temperature scale was calibrated with pure Indium (T_m = 156.6 °C).

Permeation measurements were performed at 20 °C for helium (He) and carbon dioxide (CO_2) with respective kinetic diameters of 2.6 and 3.3 Å [70]. The CER-based samples with a useful area of 3 cm^2 and a constant thickness around 150 µm were placed between the upstream and downstream compartments of the permeation cell. A secondary vacuum desorption step was performed prior to each permeation experiment. The permeation measurements were carried out under an upstream pressure, P_1, equal to 3 bars. The downstream pressure, P_2, was measured as a function of time. The permeability coefficient, P, was calculated from the slope of the linear time dependence of P_2 in a steady state, and the diffusion coefficient, D, was deduced from the time lag, θ, as determined by the extrapolation of the steady-state line on the time axis (Equation (4)):

$$D = \frac{L^2}{6\theta} \quad (4)$$

where L is the film thickness [70]. D was expressed in cm^2·s^{-1} and P in barrer (with 1 barrer = 10^{-10} $cm^3_{STP}\ cm\ /(cm^2\ s\ cm_{Hg})$).

Water sorption isotherms of the different films were determined at 25 °C by using the dynamic vapor sorption analyzer, DVS Advantage (London, United Kingdom). Each sample was predried in the DVS Advantage by exposure to dry nitrogen until the equilibrated dry mass was obtained (m_0). A partial pressure of vapor (Pi) was then established within the apparatus by mixing controlled amounts of dry and saturated nitrogen and the mass of the sample (m_t) was followed as a function of time. The mass of the sample at equilibrium (m_{eq}) was considered to be reached when changes in mass with time (dm/dt) were lower than 2.10^{-4} mg·min^{-1} for at least 5 min. Then, vapor pressure was increased in suitable activity (a_w: 0, 0.2, 0.5, 0.7, and 0.9, respectively). The value of the mass gain at equilibrium (G) was defined by Equation (5):

$$G = \frac{m_{eq} - m_0}{m_0} \quad (5)$$

Preprints (www.preprints.org) | NOT PEER-REVIEWED | Posted: 15 November 2023 doi:10.20944/preprints202311.0954.v1

For each water activity (a_w), it permitted to plot the water sorption isotherm. The precision on the values of G was estimated to be better than 5%.

The diffusion coefficient (D) was determined according to Equation (6) [70]:

$$D = \frac{0.04909 \cdot L^2}{t_{1/2}} \quad (6)$$

where $t_{1/2}$ is the half sorption time and L is the sample thickness.

3. Results and Discussions

It is well known that cyanate groups of CERs can readily react with hydrogen-containing functional groups, such as -OH, -NH_2, and -NH-, the reaction with -NH_2 and -NH- groups occurring at temperature of ~30 °C and ~65°C, respectively [65,66]. Recently, these reactions have been applied for the chemical incorporation of different functionalized nanofillers into *in-situ* growing CER networks to create high performance thermostable CER-based nanocomposites [40,46–48,50,51]. Cho et al. [50] confirmed chemical incorporation of amino-POSS into the CER (PT-30) network through the reaction of –O–C≡N groups of CER with -NH_2 groups of amino-POSS with formation of RNHC(=NH)OR fragments that were evidenced by FTIR with a stretching band at 1640 cm^{-1}. In a previous work [40], some of us observed the same band as well in the cured CER/amino-MMT nanocomposites.

In the present work, the initial stage of amino-POSS chemical grafting or incorporation into the CER network is schematically shown in **Figure 1**. Due to differences in the functionality of POSS nanoparticles, it is possible to envision a large variety in the design of the synthesized CER/amino-POSS nanocomposites.

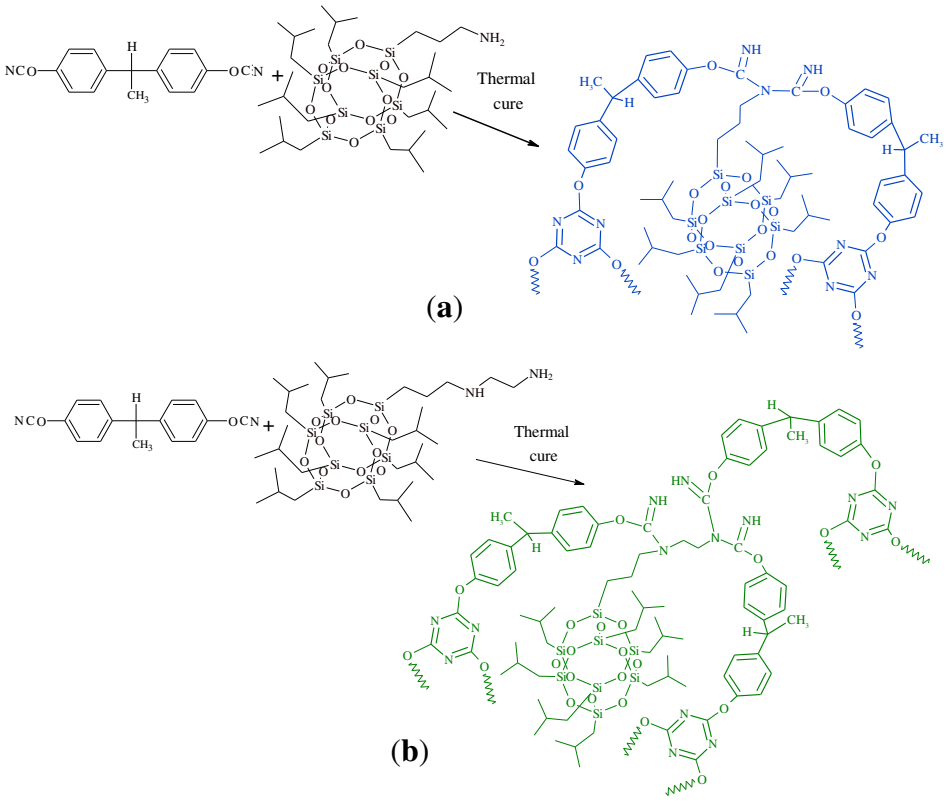

Preprints (www.preprints.org) | NOT PEER-REVIEWED | Posted: 15 November 2023 doi:10.20944/preprints202311.0954.v1

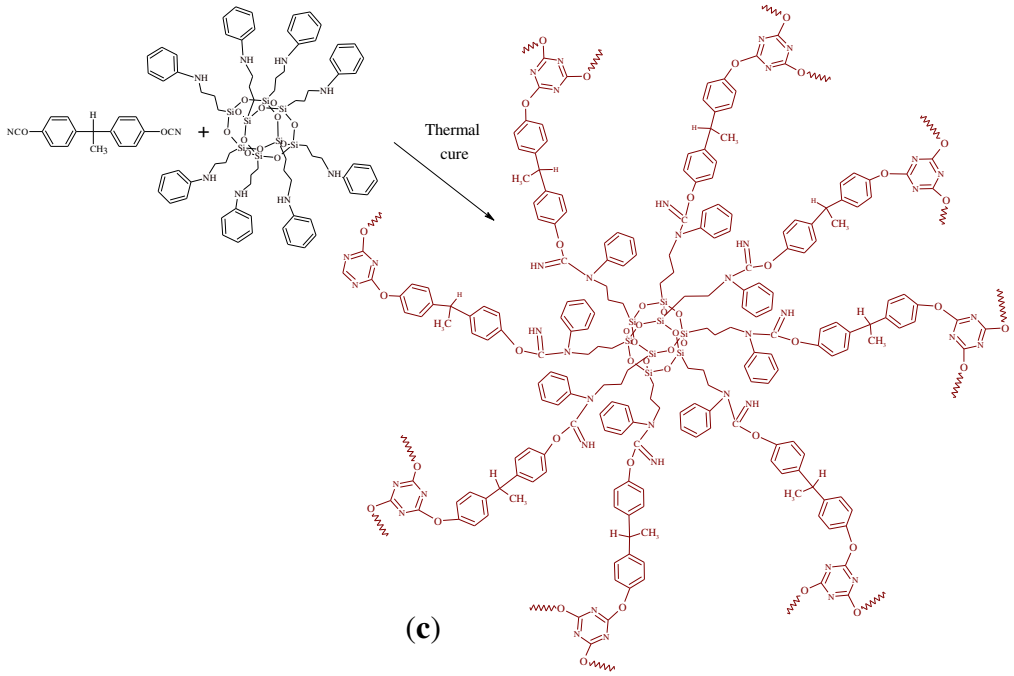

Figure 1. Schematic presentation of chemical embedding to growing CER network of different amino-POSS nanoparticles: (**a**) APIB-POSS, (**b**) AEAPIB-POSS, and (**c**) *N*PAP-POSS.

3.1. Investigation of Viscoelastic Properties by DMTA

The influence of embedding amino-POSS nanoparticles into polycyanurate networks on viscoelastic properties of the nanocomposites synthesized was investigated by using DMTA. **Figure 2** shows the temperature dependence of storage modulus, *E*' (**Fig. 2**a), loss modulus, *E*'' (**Fig. 2**b), and tan δ (**Fig. 2**c) for the neat CER network and for the nanocomposites with different amino-POSS. **Table 2** displays the corresponding viscoelastic characteristics.

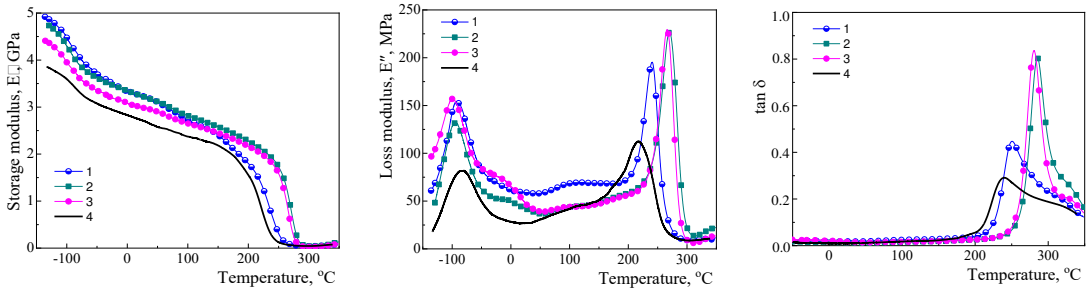

Figure 2. Temperature dependence (at 1 Hz) of (**a**) storage modulus, *E*', (**b**) loss modulus, *E*'', and (**c**) tan δ for (1) CER/APIB-POSS, (2) CER/AEAPIB-POSS, (3) CER/*N*PAP-POSS nanocomposites, and (4) neat CER network. .

Table 2. Viscoelastic properties (DMTA data) for CER/amino-POSS nanocomposites and neat CER network.

Sample	T_γ, °C	T_β, °C	T_α, °C	*E*' at 25 °C, GPa	M_c, g/mol	Surface of *E*'' peak at T_α, MPa/K	Height of tan δ (at T_α)
(1) CER/APIB-POSS	–92	–43	241	3.24	49	13.61	0.45
(2) CER/AEAPIB-POSS	–95	–11	270	3.23	83	9.83	0.81
(3) CER/*N*PAP-POSS	–99	–28	266	2.99	48	12.92	0.84
(4) Neat CER network	–85	–37	218	2.72	31	13.83	0.29

 doi:10.20944/preprints202311.0954.v1

One could see a significant influence of the addition of different types of reactive amino-POSS nanoparticles on viscoelastic properties for all the CER/amino-POSS nanocomposites synthesized. Indeed, the values of storage modulus E', the intensities of loss modulus maxima E'', and the values of α transition temperatures T_α for the CER matrix substantially changed upon introduction of the nanoparticles (see **Table 2**). All the above-mentioned changes evidenced the essential differences in hybrid CER/amino-POSS networks depending on the structure of amino-POSS used, namely the number and the reactivity of amino groups on the POSS cage surface. Amino-POSS molecules could graft from one side (in the case of APIB-POSS having one amino group) or incorporate inside (in the case of AEAPIB-POSS or *N*PAP-POSS having two or eight amino groups, respectively) the CER, thus resulting in the formation of hybrid organic-inorganic CER/POSS nanocomposites. Therefore, during the synthesis of CER/amino-POSS nanocomposites, the formation of mixed microphases with different contents of chemically grafted or incorporated amino-POSS nanoparticles in CER matrix (*i.e.* microphases with different mobility of kinetic segments of macromolecules) took place. **Figure 2** shows that loading nanofiller into CER network led to a significant increase of storage modulus, E', values in the temperature region investigated. This fact evidenced strengthening of the elastic properties associated with the polymer matrix, probably due to the well distributed relatively large nanoparticles of rigid POSS along the segments of the polymer chains as additional inorganic junctions, which hindered and restricted the movement of these segments. The uniform distribution of amino-POSS nanoparticles in the CER network without their aggregation was undoubtedly achieved due to two main reasons: (i) a sufficiently low (0.1 wt.%) nanofiller content, and (ii) the use of a special preheating procedure (before the main synthesis) for ensuring chemical interactions between the functional groups of CER and amino-POSS. Each POSS nanoparticle was thus surrounded by CER molecules transforming into polymer network at further high temperature curing, without agglomeration. As a result, the high crosslink density organic-inorganic hybrid polymer network was formed obviously without significant defects.

Recently, Zhang et al. [71] mathematically processed the curves $E''=f(T)$ for an individual CER using inverse convolution by the contributions of single relaxation processes. Four distinct peaks corresponding to main α-relaxation of higher intensity at higher temperature, and secondary γ- and β-relaxations of lower intensities at lower temperatures were detected. From **Figure 2**b, one could see that both neat CER and all CER/amino-POSS nanocomposites exhibited broad γ-relaxation assigned to the phenylene and methyl groups rotations present in the links between the planar six-member three-arm cyanurate rings of CER structure [72] with a maximum at $T \approx -85$ °C and in the temperature range from –90 °C to –100 °C, correspondingly. Secondary relaxations appeared with a maximum at T_β (from –43 to – 11°C, **Table 2**) and at $T_{\beta'} \approx 100$ °C corresponding to the β and β′ relaxations associated with the mobility of the chain fragments between the crosslink sites of the CER network [73]. One could see from **Figure 2** and **Table 2** that the CER/amino-POSS nanocomposites possessed higher values of T_α compared to the unfilled CER network. Herewith, loading the APIB-POSS into CER network resulted in a temperature shift towards higher T_α values by 18 °C, whereas addition of *N*PAP-POSS and AEAPIB-POSS sharply increased the T_α values by 44 °C and 50 ºC, respectively (see **Table 2**). Thus, the introduction of amino-POSS nanoparticles chemically grafted/incorporated into CER networks led to the formation of new hybrid crosslinking sites. As a result, the additional steric obstacles reduced the amplitude of the spatial mobility of the kinetic segments of the macromolecules of the CER network, which caused an increase in the value of T_α, thus confirming conclusions of Bershtein et al. [61] about the enhanced long-range action of the "constrained dynamics" effect. Therefore, in the presence of amino-POSS, the values of T_γ decreased, whereas the values of T_β, T_α, E', and M_c increased, evidencing that amino-POSS behaved as both thermal and mechanical antiplasticizers *i.e.*, reinforcements.

The curves for E'' and tan δ seemed to be in contradiction to what E' and T_α values showed. Indeed, an apparent increase in the E'' and tan δ peak intensities is observed for α relaxation in presence of APIB-POSS, *N*PAP-POSS, and AEAPIB-POSS, whereas a "classical" anti-plasticization effect (*i.e.* increase of T_α) would tend to the reduction of such peak intensities, since the material would be considered stiffer. However, it should be considered that not only intensity of E'' and tan δ

 doi:10.20944/preprints202311.0954.v1

peaks represent the viscoelastic behavior of a polymer, but also the peak amplitude and half-width. This is due to the fact that the main α relaxation is a heterogeneous phenomenon spanning in a range of temperatures. In order to really distinguish the influence of added nanofillers on the viscoelastic behavior of CER networks, the surfaces of the E'' peaks, representing the total modulus loss during the whole α relaxation phenomenon should be compared. The E'' peaks observed for the α relaxation were deconvoluted and integrated as detailed in the Experimental section. A single Gaussian function was considered for CER/APIB-POSS, CER/*N*PAP-POSS, and CER/AEAPIB-POSS samples whereas two Gaussian functions were considered for neat CER. The computed surfaces are summarized in **Table 2**.

Table 2 shows that CER/APIB-POSS and neat CER had similar E'' peak surfaces, that of CER/APIB-POSS being slightly lower. The reduction of the E'' peak surfaces was further observed for CER/*N*PAP-POSS, and CER/AEAPIB-POSS nanocomposites. This meant that the introduction of APIB-POSS, *N*PAP-POSS, and AEAPIB-POSS actually reduced the viscous behavior of CER, as the surface of these peaks correspond to the loss due to the viscoelastic nature of polymers during the α relaxation phenomenon, as detailed in the previous paragraph. As such, the observed increase in E'' and tan δ intensities was not due to an increase in a viscous behavior but could be correlated to a more homogeneous α relaxation phenomenon induced by the presence of the amino-based nanofiller. Finally, it could be concluded that CER/APIB-POSS, CER/*N*PAP-POSS, and CER/AEAPIB-POSS nanocomposites induced a more homogenous α relaxation phenomenon with higher T_α values, and an enhanced nanocomposite elastic behavior compared to unfilled CER network.

3.2. Investigation of Thermophysical Properties by DSC

The effect of chemically embedded amino-POSS nanoparticles into CER network on the thermophysical properties of CER/amino-POSS nanocomposites was also studied by DSC. **Figure 3** shows corresponding DSC thermograms, and **Table 3** displays the obtained thermophysical characteristics ($T_{g\ onset}$, T_g, and ΔC_p). It is noteworthy that DSC data were in a good agreement with DMTA results. For all the CER/amino-POSS nanocomposites, only a single T_g value was evidenced that meant that all the samples studied had amorphous structure. However, the $T_{g\ onset}$, T_g, and ΔC_p values of nanocomposites varied significantly depending on the functionality of amino-POSS embedded into the CER matrix. Meanwhile, introducing APIB-POSS nanoparticles led to negligible growth of T_g (by 2 °C) of polycyanurate matrix. However, adding *N*PAP-POSS and AEAPIB-POSS shifted T_g values to higher temperatures by 45 °C and 55 °C, respectively (cf. **Table 3**). Zhang et al. [71,72] attributed the increase in T_g of nanocomposites as compared to the unfilled (neat) polymer with the suppression of the polymer chain mobility by POSS molecules (cages) and Bershtein et al. [61] explained this fact by the possible manifestation of the enhanced long-range action of the "constrained dynamics" effect.

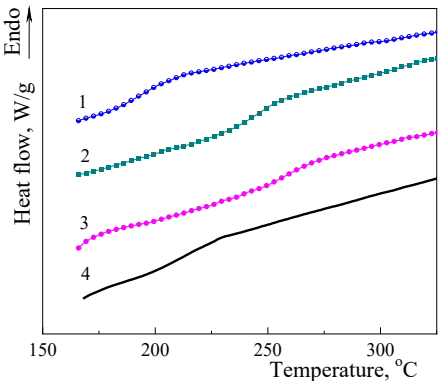

Figure 3. DSC thermograms (2nd heating scan) for (1) CER/APIB-POSS, (2) CER/AEAPIB-POSS, (3) CER/*N*PAP-POSS nanocomposites, and (4) neat CER network.

Preprints (www.preprints.org) | NOT PEER-REVIEWED | Posted: 15 November 2023 doi:10.20944/preprints202311.0954.v1

Table 3. DSC data for CER/amino-POSS nanocomposites and neat CER network.

	Sample	$T_{g\ onset}$, °C	T_g, °C	ΔC_p, J·g^{-1}·K^{-1}
(1)	CER/APIB-POSS	204	216	0.363
(2)	CER/AEAPIB-POSS	257	269	0.415
(3)	CER/*N*PAP-POSS	249	259	0.314
(4)	Neat CER network	203	214	0.351

3.3. Investigation of Thermal Stability by TGA

The effect of the different amino-POSS used on thermal stability of the nanocomposites synthesized was studied by TGA. **Figure 4** shows TGA (**Figure 4**a, in argon) and corresponding DTG (**Figure 4**b) curves for the CER/amino-POSS nanocomposites (**Figure 4**, curves 1-3) compared to that for the neat CER network (**Figure 4**, curve 4). The corresponding thermal characteristics are summarized in **Table 4**. A strong influence of even such a low content (0.1 wt.%) of the selected nanofillers on thermal stability of CER/amino-POSS nanocomposites formed *in situ* was clearly observed. Indeed, the improved thermal stability was shown when APIB-POSS or AEAPIB-POSS were used in a contrast to *N*PAP-POSS.

Two simultaneous processes could occur during CER/amino-POSS nanocomposite formation: (i) the densely crosslinked polymer network with additional hybrid inclusions/junctions was formed, due to chemical grafting/incorporation of thermostable POSS nanoparticles into the CER network that led to an improvement of thermal characteristics of CER-based nanocomposites, and (ii) some defects were generated in the CER network, due to the existence of POSS nanoparticles with diameters of 1-2 nm inside the growing CER matrix that could hinder the formation of the regular CER network and weaken its thermal properties.

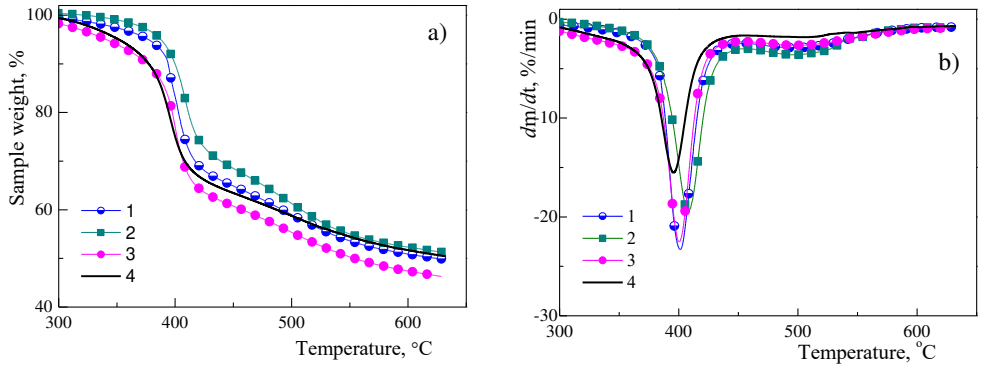

Figure 4. Typical (**a**) TGA and (**b**) DTG curves (in argon) for (1) CER/APIB-POSS, (2) CER/AEAPIB-POSS, (3) CER/*N*PAP-POSS nanocomposites, and (4) neat CER network.

Table 4. Thermal stability of CER/amino-POSS nanocomposites and neat CER network.

	Sample	$T_{d5\%}$ [(a)], °C	$T_{d\ max}$ [(b)], °C	Δm [(c)], %	m_{ash} [(d)], %
(1)	CER/APIB-POSS	377	401	23	50
(2)	CER/AEAPIB-POSS	388	408	18	51
(3)	CER/*N*PAP-POSS	341	401	23	46
(4)	Neat CER network	352	396	21	51

[(a)] $T_{d5\%}$ is the temperature of 5 % mass loss; [(b)] $T_{d\ max}$ is the temperature value of maximal degradation rate; [(c)] Δm is the mass loss at maximal degradation rate; [(d)] m_{ash} is the ash content at T = 630 °C.

One could see that neat CER and CER/amino-POSS nanocomposites were characterized by two stages of decomposition. The main stage was in a region of ~ 374-440 °C related to the degradation of cyanurate skeleton [2,3], and a second stage at 467-531 °C. The residual char was determined to be ~

Preprints (www.preprints.org) | NOT PEER-REVIEWED | Posted: 15 November 2023 doi:10.20944/preprints202311.0954.v1

46-51 % at 630 °C. Nevertheless, the thermal stability of the nanocomposites increased when only 0.1 wt.% of different amino-POSS were loaded compared to the unfilled CER matrix. Thus, one could conclude that the temperature of the intensive decomposition onset, for the unfilled CER matrix was quite high ($T_{d1\ onset}$ = 374 °C), and it increased by ≈ 9-15 °C when introducing amino-POSS nanoparticles. The temperature of maximal degradation rate $T_{d1\ max}$ shifted to higher temperatures by ≈ 5-12 °C as well depending on the functionality of the amino-POSS used. It should be pointed out that when loading both APIB-POSS with one primary amino group and *N*PAP-POSS with eight secondary amino groups into the CER matrix, all the thermal characteristics increased by 5-10 °C compared to the neat CER network. More interestingly, the greatest impact on thermal stability (increasing by 12-15 °C) was observed with loading of AEAPIB-POSS with one secondary and one primary amino groups. It was obvious that primary amino group had a reactivity higher than that of secondary amino group, which resulted in a higher degree of POSS nanoparticles grafting to CER network. In conclusion, the highest effect was logically observed for AEAPIB-POSS, where the effect of primary amino group was further enhanced by the presence of secondary amino group.

3.4. Investigation of Gas Transport Properties

The specific surface area (*S*) values for all the synthesized samples were determined from nitrogen adsorption/desorption isotherms by using the BET method. The *S* value for the neat CER network was equal to around 62 m²/g, whereas the introduction of amino-POSS nanoparticles increased the values of specific surface area to 105, 108, and 272 m²/g for CER/APIB-POSS, CER/*N*PAP-POSS, and CER/AEAPIB-POSS nanocomposites, respectively (**Figure 5**a).

Gas transport properties for neat CER and CER/amino-POSS nanocomposites were determined, and the results obtained are depicted in **Figure 5**b. He and CO_2 permeability increased respectively by ≈ 2 and 3.5-4 times, and diffusion coefficient of CO_2 increased approximately twice for CER/amino-POSS nanocomposites in comparison with the neat CER network. These results were in a good correlation with the above reported data on the specific surface area. Obviously, the introduction of amino-POSS nanoparticles led to increasing free volume of the nanocomposites studied that represented additional diffusion paths for gas transport [74,75]. Formation of looser structure in hybrid CER-based nanocomposite networks was also confirmed by increasing ΔC_P values (see DSC data in **Table 3**) and increasing M_c values (see DMTA data in **Table 2**) with incorporation of amino-POSS nanoparticles into the CER network.

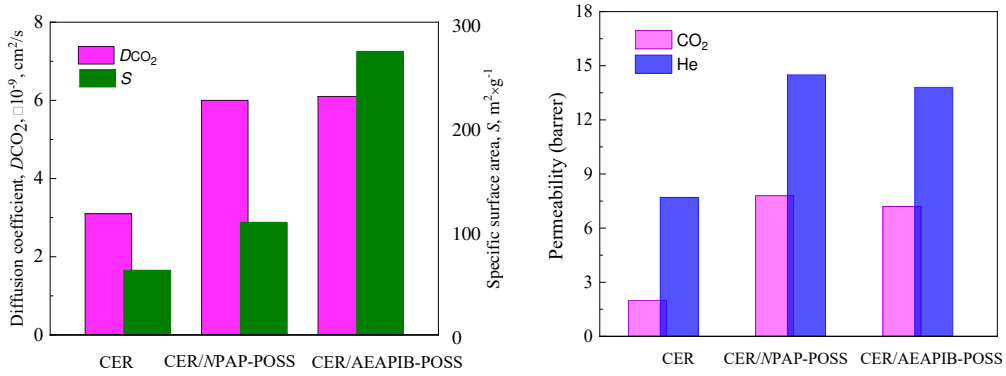

Figure 5. Specific surface area (**a**), diffusion coefficient (**a**), and permeability coefficient (**b**) for neat CER and CER/amino-POSS films under investigation.

Figure 6a displays the evolution of the water uptake (*G*) for the neat CER network and CER/*N*PAP-POSS and CER/AEAPIB-POSS nanocomposites. The water uptakes remained rather low (less than 3 wt.%) as usually observed in the case of thermosets [74,76]. The water sorption isotherms were of BET II type. The slight curvature observed at low water activity (below a_w=0.2) was related to the presence of water molecules strongly linked to the polar groups contained in the materials, and

Preprints (www.preprints.org) | NOT PEER-REVIEWED | Posted: 15 November 2023 doi:10.20944/preprints202311.0954.v1

the positive deviation from linearity evidenced at high water activity indicated a water clustering phenomenon. One could observe a small decrease in the water uptake at high water activity for CER/amino-POSS nanocomposite samples compared to neat CER, meaning that the presence of POSS hindered water clustering (**Fig. 6**a). The evolution of the water diffusion coefficient (*D*) values of the samples studied as a function of the water activity is presented in **Figure 6**b. The *D* values measured at low water activity were higher for the CER/amino-POSS films with respect to neat CER. This trend was the same as that observed for gas transport, and it was related to the higher free volume contained in the CER/amino-POSS films. It could also be observed that the profile of water diffusion of neat CER network was different from that of CER/*N*PAP-POSS and CER/AEAPIB-POSS. It seemed that the higher clustering phenomenon observed at high water activity for neat CER induced a slight plasticization effect with an increase in *D* values, whereas the more limited clustering effect taking place in CER/amino-POSS films led to a small decrease in *D* values, as usually observed in networks [76]. However, *D* variations remained small in both cases.

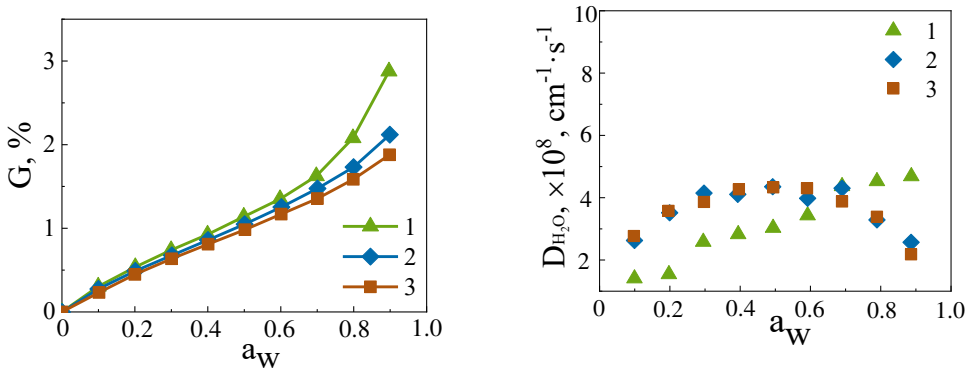

(**a**) (**b**)

Figure 6. Water sorption (*G*) isotherms (**a**) and evolution of the water diffusion (*D*) (***b***) for neat CER (1), CER/*N*PAP-POSS (2), and CER/AEAPIB-POSS (3) nanocomposites as a function of water activity.

4. Conclusions

Nanocomposites of cyanate ester resin (CER) filled with different types of reactive amino functionalized POSS were synthesized and characterized. It was found that the addition of a small quantity (0.1 wt.%) of amino-POSS chemically grafted to the CER network led to a significant increase in the thermal stability of the CER matrix. Namely, the degradation temperature onset, $T_{d\,onset}$, and the temperature of maximal degradation rate, $T_{d\,max}$, shifted to higher temperatures by ≈ 12-15 °C, depending on the type of amino-POSS. The significant growth of glass transition and α relaxation temperatures, T_g and T_α, by 45-55 °C of the CER matrix with loading of nanofillers was demonstrated by means of DSC and DMTA, respectively. The essential increase in storage modulus values in the temperature region investigated was observed as well. Formation of looser structures in hybrid CER-based nanocomposite networks was also confirmed by increasing ΔC_P (DSC data) and increasing M_c values (DMTA data) with incorporation of amino-POSS nanoparticles into the CER network.

It was shown that CER/amino-POSS nanocomposites possessed specific surface area, gas permeability (CO_2, He), and diffusion coefficients (CO_2 and H_2O at low activity) higher than that for neat CER. The efficiency of amino-functionalized POSS in improving the thermal and gas transport properties of the CER/amino-POSS nanocomposites increased in a raw of POSS containing one primary amino group (APIB-POSS) < eight secondary amino groups (*N*PAP-POSS) < one secondary and one primary amino groups (AEAPIB-POSS). APIB-POSS had the least strong effect, since it could form covalent bonds with CER network only by reaction of one $-NH_2$ group. *N*PAP-POSS could connect to CER network through reaction of 8 –NH– groups but reactivity of –NH– groups was quite low, so its effect was slightly diminished. AEAPIB-POSS had the strongest effect, since it could easily

be incorporated into CER network *via* reaction of one –NH_2 and one –NH– groups with –O–C≡N groups of CER.

Author Contributions: Conceptualization, O.G., A.F., and D.G.; methodology, O.G., E.E., and A.F.; validation, E.E., D.S., and O.S.; investigation, O.S., D.S., F.G., and A.R.A.; formal analysis, O.G., A.F., O.S., and D.G.; writing—original draft preparation, O.S., E.E., and A.R.A.; writing—review and editing, O.G., A.F., and D.G.; visualization, D.S. and F.G.; supervision, A.F. and D.G.; project administration, A.F. and D.G. All authors have read and agreed to the published version of the manuscript.

Funding: This research received no external funding.

Institutional Review Board Statement: Not applicable.

Data Availability Statement: Not applicable.

Acknowledgments: The work was supported by the National Academy of Sciences of Ukraine (NASU) and the "Centre National de la Recherche Scientifique" (CNRS) through French-Ukrainian International Research Projects on Nanoporous Thermostable Polymer Materials "LIA POLYNANOPOR" and "IRP POLYTHERMAT".

Conflicts of Interest: The authors declare no conflict of interest.

References

1. Shimp, D.A.; Christenson, J.R.; Ising S.J. Cyanate esters. An emerging family of versatile composite resins. In Proceedings of the 34th Annual International SAMPE Symposium, Reno, Nevada, USA, 8-11 May 1989.
2. Hamerton, I. [ed.] *Chemistry and technology of cyanate ester resins.* Chapman & Hall: London, UK, 1994; 357 p. DOI: 10.1007/978-94-011-1326-7.
3. Hamerton, I.; Hay, J.N. Recent technological developments in cyanate ester resins. *High Perfom. Polym.*, **1998**, 10, 163–174. DOI: 10.1088/0954-0083/10/2/001.
4. Nair, C.P.R.; Mathew, D.; Ninan, K.N. Cyanate Ester Resins, Recent Developments. *Adv. Polym. Sci.*, **2000**, 155, 1–99. DOI: 10.1007/3-540-44473-4_1.
5. Fainleib A. [ed.] *Thermostable polycyanurates. Synthesis, modification, structure and properties*. Nova Science Publisher: New York, USA, 2010; 362 p.
6. McConnell, V.P. Resins for the Hot Zone, Part II: BMIs, CEs, benzoxazines and phthalonitriles. *High Perform. Composites*, **2009**, 21, 49–54. https://www.compositesworld.com/articles/resins-for-the-hot-zone-part-ii-bmis-ces-benzoxazines-and-phthalonitriles
7. Bershtein, V.A.; Egorova, L.M.; Ryzhov, V.P.; Yakushev, P.N.; Fainleib, A.M.; Shantalii, T.A.; Pissis P. Structure and segmental dynamics heterogeneity in hybrid polycyanurate-polyurethane networks. *J. Macromol. Sci., Phys. B.*, **2001**, 40, 105-131. DOI: 10.1081/MB-100000057
8. Fainleib, A.; Grigoryeva, O.; Hourston, D. Synthesis of inhomogeneous modified polycyanurates by reactive blending of bisphenol A dicyanate ester and polyoxypropylene glycol. *Macromol. Symp.*, **2001**, 164, 429-442. DOI: 10.1002/1521-3900(200102)164:1<429::AID-MASY429>3.0.CO;2-I
9. Fainleib, A.M.; Grigoryeva, O.P.; Hourston, D.J. Structure-properties relationships for bisphenol A polycyanurate network modified with polyoxytetramethylene glycol. *Int. J. Polym. Mat.*, **2002**, 51(1-2), 57-75. DOI: 10.1080/00914030213025
10. Iijima, T.; Kunimi, T.; Oyama, T.; Tomoi, M. Modification of cyanate ester resin by soluble polyarylates. *Polym. Int.*, **2003**, 52, 773–782. DOI: 10.1002/pi.1146.
11. Hwang, J.W.; Park, S.D.; Cho, K.; Kim, J.K.; Park, C.E. Toughening of cyanate ester resins with cyanated polysulfones. *Polymer*, **1997**, 38, 1835–1843. DOI: 10.1016/S0032-3861(96)00715-X
12. Kim, Y.S.; Min, H.S.; Choi, W.J.; Kim, S.C. Dynamic mechanical modeling of PEI/dicyanate semi-IPNs. *Polym. Eng. Sci.*, **2000**, 40, 665–675. DOI: 10.1002/pen.11197
13. Harismendy, I.; Rio, M.D.; Marieta, C.; Gavalda, J.; Mondragon, I. Dicyanate ester-polyetherimide semi-interpenetrating polymer networks. II. Effects of morphology on the fracture toughness and mechanical properties. *J. Appl. Polym. Sci.*, **2001**, 80, 2759–2767. DOI: 10.1002/app.1391
14. Liu, J.; Ding, N.; Xu, R.; He, Q.; Shen, J.; Hu, B. Cyanate ester resin modified by hydroxyl-terminated polybutadiene: morphology, thermal, and mechanical properties. *Polym. Eng. Sci.*, **2011**, 51, 1404–1408. DOI: 10.1002/pen.21952
15. Fainleib, A.; Kozak, N.; Grigoryeva, O.; Nizelskii, Yu.; Gritsenko, V.; Pissis, P.; Boiteux, G. Structure-thermal property relationships for polycyanurate-polyurethane linked interpenetrating polymer networks. *Polym. Degrad. Stab.*, **2002**, 76, 393-399. DOI: 10.1016/S0141-3910(02)00031-9
16. Kim, Y.S; Kim, S.C. Properties of polyetherimide/dicyanate semi-interpenetrating polymer network having the morphology spectrum. *Macromolecules*, **1999**, 32, 2334–2341. DOI: 10.1021/ma981083v

17. Bartolotta, A.; Di Marco, G.; Lanza, M.; Carini, G.; D'Angelo, G.; Tripodo, G.; Fainleib, A.; Danilenko, I.; Grytsenko, V.; Sergeeva, L. Thermal and mechanical properties of simultaneous and sequential full-interpenetrating polymer networks. *Mater. Sci. Eng. A.*, **2004**, 370, 288-292. DOI: 10.1016/j.msea.2003.07.017
18. Iijima, T.; Katsurayama, S.; Fukuda, W.; Tomoi, M.J. Modification of cyanate ester resin by poly(ethylene phthalate) and related copolyesters. *J. Appl. Polym. Sci.*, **2000**, 76, 208–219. DOI: 10.1002/(SICI)1097-4628(20000411)76:2<208::AID-APP10>3.0.CO;2-N
19. Cao, Z.Q.; Mechin, F.; Pascault, J.P. Influence of cure cycles on morphologies and properties of rubber- or thermoplastic-modified cyanate ester networks. *Polym. Mater. Sci. Eng*., **1995**, 71, 752–753.
20. Seminovych, G.M.; Fainleib, A.M.; Slinchenko, E.A.; Brovko, A.A.; Sergeeva, L.M.; Dubkova, V.I. Influence of carbon fibre on formation kinetics of cross-linked copolymer from bisphenol A dicyanate and epoxy olygomer. *React. Funct. Polym*., **1999**, 40, 281-288. DOI: 10.1016/S1381-5148(98)00049-2
21. Hwang, J.W.; Cho, K.; Yoon, T.H.; Park, C.E. Effects of molecular weight of polysulfone on phase separation behavior for cyanate ester/polysulfone blends. *J. Appl. Polym. Sci*., **2000**, 77, 921–927. DOI:10.1002/(SICI)1097-4628(20000725)77:4<921::AID-APP28>3.0.CO;2-4
22. Chang, J.-Y.; Hong, J.-L. Morphology and fracture toughness of poly(ether sulfone)-blended polycyanurates. *Polymer*, **2000**, 41, 4513-4521. DOI:10.1016/S0032-3861(99)00616-3
23. Hwang, J.W.; Cho, K.; Park, C.E.; Huh, W. Phase separation behavior of cyanate ester resin/polysulfone blends. *J. Appl. Polym. Sci.*, **1999**, 74, 33–45. DOI: 10.1002/(SICI)1097-4628(19991003)74:1<33::AID-APP4>3.0.CO;2-Q
24. Recalde, I.B.; Campos, A.; Mondragon, I.; Gomez, C.M. Miscibility and kinetic behaviour of cyanate resin/polysulfone blends. *Macromol. Symp*., **2001**, 174, 175–185. DOI:10.1002/1521-3900(200109)174:1%3C175::AID-MASY175%3E3.0.CO;2-G
25. Srinivasan, S.A.; Rau, A.V.; Loos, A.C.; McGrath, J.E. Toughened cyanate ester networks as matrix resin for carbon fiber composites. *Polym. Mater. Sci. Eng*., **1995**, 71, 750–751.
26. Srinivasan, S.A.; McGrath, J.E. Amorphous phenolphthalein-based poly(arylene ether)- modified cyanate ester networks: Effect of thermal cure cycle on morphology and toughenability. *J. Appl. Polym. Sci.*, **1997**, 64, 167–178. DOI: 10.1002/(SICI)1097-4628(19970404)64:1<167::AID-APP15>3.0.CO;2-1
27. Rau, A.V.; Srinivasan, S.A.; McGrath, J.E.; Loos, A.C. Resin transfer molding (RTM) with toughened cyanate ester resin systems. *Polym. Comp*., **1998**, 19, 166–179. DOI: 10.1002/pc.10088
28. Marieta, C.; Rio, M.D.; Harismendy, I.; Mondragon, I. Effect of the cure temperature on the morphology of a cyanate ester resin modified with a thermoplastic: characterization by atomic force microscopy. *Eur. Polym. J*., **2000**, 36, 1445–1454. DOI: 10.1016/S0014-3057(99)00203-7
29. Chang, J.-Y.; Hong, J.-L. Polar interaction in a cyanated poly(ether sulfone)-modified polycyanurate. *Polymer*, **1998**, 39, 7119–7122. DOI: 10.1016/S0032-3861(98)00185-2
30. Hillermeier, R.W.; Seferis, J.C. Environmental effects on thermoplastic and elastomer toughened cyanate ester composite systems. *J. Appl. Polym. Sci.*, **2000**, 77, 556–567. DOI: 10.1002/(SICI)1097-4628(20000718)77:3<556::AID-APP11>3.0.CO;2-9
31. Brown, J.M.; Srinivasan, S.A.; Rau, A.V.; Ward, T.C.; McGrath, J.E.; Loos, A.C.; Hood, D.; Kranbeuhl, D.E. Production of controlled networks and morphologies in toughened thermosetting resins using real-time, in situ cure monitoring. *Polymer*, **1996**, 37, 1691–1696. DOI: 10.1016/0032-3861(96)83720-7
32. Fainleib, A.M.; Sergeeva, L.M.; Novikova, T.I.; Shantalii, T.A. Synthesis, structure and some properties of the polycyanurate-polyurethane semi-IPNs. *Polym. Mater. Sci. Eng*., **1992**, 66, 131-132.
33. Bartolotta, A.; Di Marco, G.; Lanza, M.; Carini, G.; D'Angelo, G.; Tripodo, G.; Fainleib, A.M.; Slinchenko, E.A.; Privalko, V.P. Molecular mobility in semi-IPNs of linear polyurethane and heterocyclic polymer networks. *J. Adhes*., **1997**, 64, 269-286. DOI:10.1080/00218469708010543
34. Balta Calleja, F.J.; Privalko, E.G.; Sukhorukov, D.I.; Fainleib, A.M.; Sergeeva, L.M.; Shantalii, T.A.; Shtompel, V.I.; Monleon Pradas, M.; Gallego Ferrer, G.; Privalko ,V.P. Structure-properties relationships for cyanurate-containing, full interpenetrating polymer networks. *Polymer*, **2000**, 41, 4699-4707. DOI:10.1016/S0032-3861(99)00504-2
35. Maroulas, P.; Kripotou, S.; Pissis, P.; Fainleib, A.; Bei, I.; Bershtein, V.; Gomza, Yu. Molecular mobility in polycyanurate/clay nanocomposites studied by dielectric techniques. *J. Compos. Mater*., **2009**, 43, 943–958. DOI: 10.1177/0021998308097736
36. Anthoulis, G.I.; Kontou, E.; Fainleib, A.; Bei, I. Polytetramethylene glycol-modified polycyanurate matrices reinforced with nanoclays: synthesis and thermomechanical performance. *Mech. Comp. Mater*., **2009**, 45, 175–182. DOI:10.1007/s11029-009-9073-x
37. Bershtein, V.A.; Fainleib, A.M.; Pissis, P.; Bei, I.M.; Dalmas, F.; Egorova, L.M.; Gomza, Yu.P.; Kripotou, S.; Maroulas, P.; Yakushev, P.N. Polycyanurate-organically modified montmorillonite nanocomposites: Structure-dynamics-properties relationships. *J. Macromol. Sci. Part B: Polym. Phys*., **2008**, 47, 555–575. DOI: 10.1080/00222340801955545

38. Anthoulis, G.I.; Kontou, E.; Fainleib, A.; Bei, I.; Gomza, Yu. Synthesis and characterization of polycyanurate/montmorillonite nanocomposites. *J. Polym. Sci. Part B Polym. Phys*., **2008**, 46, 1036–1049. DOI: 10.1002/polb.21436
39. Wooster, T.J.; Abrol, S.; MacFarlane, D.R. Rheological and mechanical properties of percolated cyanate ester nanocomposites. *Polymer*, **2005**, 46, 8011–8017. DOI: 10.1016/j.polymer.2005.06.106
40. Bershtein, V.; Fainleib, A.; Egorova, L.; Gusakova, K.; Grigoryeva, O.; Kirilenko, D.; Konnikov, S.; Ryzhov, V.; Yakushev, P.; Lavrenyuk, N. The impact of ultra-low amounts of amino-modified MMT on dynamics and properties of densely cross-linked cyanate ester resins. *Nanoscale Res. Lett*., **2015**, 10, 165 (p. 1-15). DOI: 10.1186/s11671-015-0868-5
41. Dominguez, D.D.; Laskoski, M.; Keller, T.M. Modification of oligomeric cyanate ester polymer properties with multi-walled carbon nanotube-containing particles. *Macromol. Chem. Phys*., **2009**, 210, 1709–1716. DOI: 10.1002/macp.200900343
42. Fainleib, A.; Bardash, L.; Boiteux, G. Catalytic effect of carbon nanotubes on polymerization of cyanate ester resins. *eXPRESS Polym. Lett*., **2009**, 3, 477–482. DOI: 10.3144/expresspolymlett.2009.59
43. Tang, Y.; Liang, G.; Zhang, Z.; Han, J. Performance of aluminum borate whisker reinforced cyanate ester resin. J. *Appl. Polym. Sci*., **2007**, 106, 4131–4137. DOI: 10.1002/app.26118
44. Ren, P.; Liang, G.; Zhang, Z.; Lu, T. ZnO whisker reinforced M40/BADCy composite. *Compos. Part A, Appl. Sci. Manuf*., **2006**, 37, 46-53. DOI: 10.1016/j.compositesa.2005.05.018
45. Badrinarayanan, P.; Rogalski, M.K.; Kessler, M.R. Carbon fiber-reinforced cyanate ester/nano-ZrW2O8 composites with tailored thermal expansion. *Appl. Mater. Interfaces*, **2012**, 4, 510–517. DOI: 10.1021/am201165q.
46. Bershtein, V.; Fainleib, A.; Kirilenko, D.; Yakushev, P.; Gusakova, K.; Lavrenyuk, N.; Ryzhov, V. Dynamics and properties of high performance amorphous polymer subnanocomposites with ultralow silica content and quasi-regular structure. *Polymer*, **2016**, 103, 36-40. DOI: 10.1016/j.polymer.2016.09.020
47. Bershtein, V.; Fainleib, A.; Gusakova, K.; Kirilenko, D.; Yakushev, P.; Egorova, L.; Lavrenyuk, N.; Ryzhov, V. Silica subnanometer-sized nodes, nanoclusters and aggregates in cyanate ester resin-based networks: structure and properties of hybrid subnano- and nanocomposites. *Eur. Polym. J*., **2016**, 85C, 375-389. DOI: 10.1016/j.eurpolymj.2016.10.047
48. Bershtein, V.; Fainleib, A.; Kirilenko, D.; Yakushev, P.; Gusakova, K.; Lavrenyuk, N.; Ryzhov, V. Incorporating silica into cyanate ester-based network by sol-gel method: Structure and properties of subnano- and nanocomposite. *AIP Conference Proceedings*, **2016**, 1736, 020045 (p. 1-4). DOI: 10.1063/1.4949620.
49. Liang, K.; Li, G.; Toghiani, H.; Koo, J.H.; Pittman, C.U.Jr. Cyanate ester/polyhedral oligomeric silsesquioxane (POSS) nanocomposites: Synthesis and characterization. *Chem. Mater*., **2006**, 18, 301–312. DOI: 10.1021/cm051582s
50. Cho, H.-S.; Liang, K.; Chatterjee, S.; Pittman, C.U.Jr. Synthesis, morphology, and viscoelastic properties of polyhedral oligomeric silsesquioxane nanocomposites with epoxy and cyanate ester matrices. *J. Inorg. Organomet. Polym*., **2005**, 15, 541–543. DOI: 10.1007/s10904-006-9008-0
51. Pittman, C.U.Jr.; Li, G.-Z.; Ni, H. Hybrid inorganic/organic crosslinked resins containing polyhedral oligomeric silsesquioxanes. *Macromol. Symp*., **2003**, 196, 301–325. DOI: 10.1002/masy.200390170
52. Liang, K.; Toghiani, H.; Pittman, C.U.Jr. Synthesis, morphology and viscoelastic properties of epoxy/polyhedral oligomeric silsesquioxane (POSS) and epoxy/cyanate ester/POSS nanocomposites. *J. Inorg. Organomet. Polym*., **2011**, 21, 128–142. DOI: 10.1007/s10904-010-9436-8
53. Liang, K.; Toghiani, H.; Li, G.; Pittman, C.U. Jr. Synthesis, morphology, and viscoelastic properties of cyanate ester/polyhedral oligomeric silsesquioxane nanocomposites. *J. Polym. Sci. Part A: Polym. Chem*., **2005**, 43, 3887–3898. DOI: 10.1002/pola.20861
54. Wright, M.E.; Petteys, B.J.; Guenthner, A.J.; Yandek, G.R.; Baldwin, L.C.; Jones, C.; Roberts, M.J. Synthesis and chemistry of a monotethered-POSS bis(cyanate) ester: Thermal curing of micellar aggregates leads to discrete nanoparticles. *Macromolecules*, **2007**, 40, 3891–3894. DOI: 10.1021/ma0703507
55. Lin, Y.; Jin, J.; Song, M.; Shaw, S.J.; Stone, C.A. Curing dynamics and network formation of cyanate ester resin/polyhedral oligomeric silsesquioxane nanocomposites. *Polymer*, **2011**, 52, 1716–1724. DOI: 10.1016/j.polymer.2011.02.041
56. Ma, J.; Li, Q. Gelation behavior, morphology, thermal and viscoelastic properties of epoxy-cyanate ester/polyhedral oligomeric silsesquioxane (POSS) nanocomposites. *Adv. Mater. Res*., **2006**, 11-12, 323–326. DOI: 10.4028/www.scientific.net/amr.11-12.323
57. Lu, T.; Liang, G.; Guo, Z. Preparation and characterization of organic–inorganic hybrid composites based on multiepoxy silsesquioxane and cyanate resin. *J. Appl. Polym. Sci*., **2006**, 101, 3652–3658. DOI: 10.1002/app.22743
58. Bershtein, V.; Fainleib, A.; Yakushev, P.; Egorova, L.; Grigoryeva, O.; Ryzhov, V.; Starostenko, O. Thermostable cyanate ester resins and POSS-containing nanocomposites: influence of matrix chemical structure on their properties. *Polym. Adv. Technol.*, **2016**, 27, 339–349. DOI: 10.1002/pat.3645

59. Zhang, Z.; Liang, G.; Wang, X. Epoxy-functionalized polyhedral oligomeric silsesquioxane/cyanate ester resin organic–inorganic hybrids with enhanced mechanical and thermal properties. *Polym. Int*., **2014**, 63, 552–559. DOI: 10.1002/pi.4557
60. Starostenko, O.; Bershtein, V.; Fainleib, A.; Egorova, L.; Grigoryeva, O.; Sinani, A.; Yakushev, P. Thermostable polycyanurate-polyhedral oligomeric silsesquioxane hybrid networks: synthesis, dynamics and thermal behavior. *Macromol. Symp*., **2012**, 316, 90-96. DOI: 10.1002/masy.201250612
61. Bershtein, V.; Fainleib, A.; Egorova, L.; Grigoryeva, O.; Kirilenko, D.; Konnikov, S.; Ryzhov, V.; Starostenko, O.; Yakushev, P.; Yagovkina, M.; Saiter, J.-M. The impact of ultra-low amounts of introduced reactive POSS nanoparticles on structure, dynamics and properties of densely cross-linked cyanate ester resins. *Eur. Polym. J*., **2015**, 67, 128-142. DOI: 10.1016/j.eurpolymj.2015.03.022
62. Starostenko, O.; Grigoryeva, O.; Fainleib, A.; Saiter, J.M.; Youssef, B.; Grande, D. Effect of epoxy-functionalized POSS on thermal stability of nanocomposites based on crosslinked polycyanurates. *Polimernyi Zhurnal*, **2014**, 36, 233-244. http://polymerjournal.kiev.ua/wp-content/uploads/2016/06/3_233_244Starostenko.pdf
63. Grigoryeva, O.P.; Starostenko, O.N.; Gusakova, K.G.; Fainleib, A.M.; Saiter, J.M; Youssef, B.; Grande, D. Effect of epoxyfunctionalized POSS on chemical structure and viscoelastic properties of polycyanurate based nanocomposites. *Polimernyi Zhurnal*, **2014**, 36, 341-351. http://nbuv.gov.ua/UJRN/Polimer_2014_36_4_4
64. Bershtein, V.; Fainleib, A.; Yakushev, P.; Kirilenko, D.; Egorova, L.; Grigoryeva, O.; Ryzhov, V.; Starostenko, O. High performance multifunctional cyanate ester oligomer-based network and epoxy-POSS containing nanocomposites: Structure, dynamics, and properties. *Polym. Compos*., **2020**, 41, 1900-1912. DOI: 10.1002/pc.25506
65. Grigat, E.; Pütter, R. Umsetzung von cyansäureestern mit amino- bzw. Imino-gruppenhaltigen substanzen. *Chem. Ber*., **1964**, 97(11), 3027-3035. DOI: 10.1002/cber.19640971110
66. Bauer, J.; Bauer, M. Curing of cyanates with primary amines. *Macromol. Chem. Phys*., **2001**, 202, 2213-2220. DOI: 10.1002/1521-3935(20010701)202:11<2213::AID-MACP2213>3.0.CO;2-B
67. Hallary, J.-L.; Lauprêtre, F.; Monnerie, L. [ed.] *Polymer Materials, Macroscopic Properties and Molecular Interpetrations*; John Wiley & Sons: Hoboken, NJ, USA, 2010; 432 p.
68. Flory, P. J. [ed.] *Principles of Polymer Chemistry*. Cornell University Press: Ithaca, NY, USA,1953; 688 p.
69. Gregg, S.J.; Sing, K.S.W. *Adsorption, Surface Area and Porosity*. Academic Press: London, New York, 1982; 303 p. ISBN: 0123009561 9780123009562.
70. Crank, J.; Park, G.S. *Diffusion in Polymers*. Academic Press: London, New York, 1968; 452 p. DOI: 10.1002/app.1970.070140623
71. Zhang, Z.; Liang, G.; Wang, J.; Ren, P. Epoxy/POSS organic-inorganic hybrids: viscoelastic, mechanical properties and micromorphologies. *Polym. Compos*., **2007**, 28, 175–179. DOI: 10.1002/pc.20281
72. Zhang, Z.; Liang, G.; Wang, X.; Adhikari, S.; Pei, J. Curing behavior and dielectric properties of amino-functionalized polyhedral oligomeric silsesquioxane/cyanate ester resin hybrids. *High Perform. Polym*., **2013**, 25, 427-435. DOI: 10.1177/0954008312469234
73. Vashchuk, A.; Rios de Anda, A.; Starostenko, O.; Grigoryeva, O.; Sotta, P.; Rogalsky, S.; Smertenko, P.; Fainleib, A.; Grande, D. Structure-property relationships in nanocomposites based on cyanate ester resins and 1-heptyl pyridinium tetrafluoroborate ionic liquid. *Polymer*, **2018**, 148, 14-26. DOI: 10.1016/j.polymer.2018.06.015
74. Damian, C.; Escoubes, M.; Espuche, E. Gas and water transport properties of epoxy-amine networks: influence of crosslink density. *J. Appl. Polym. Sci.*, **2001**, 80, 2058-2066. DOI: 10.1002/app.1305
75. Damian, C.; Espuche, E.; Escoubes, M. Influence of three ageing types (thermal oxidation, radiochemical and hydrolytic ageing) on the structure and gas transport properties of epoxy-amine networks. *Polym. Degrad. Stab*., **2001**, 72, 447-458. DOI: 10.1016/S0141-3910(01)00045-3
76. Dolmaire, N.; Méchin, F.; Espuche, E.; Pascault, J.P. Modification of a hydrophilic linear polyurethane by crosslinking with a polydimethylsiloxane: influence of the crosslink density and of the hydrophobic/hydrophilic balance on the water transport properties. *J. Polym. Sci. B Polym. Phys*., **2006**, 44, 48-61. DOI: 10.1002/polb.20675.